

Hollow PbWO<sub>4</sub> Nanospindles via a Facile Sonochemical RouteJun Geng,<sup>†‡</sup> Jun-Jie Zhu,<sup>\*†</sup> Du-Juan Lu,<sup>†</sup> and Hong-Yuan Chen<sup>†</sup>

Department of Chemistry, Key Laboratory of Analytical Chemistry for Life Science, Nanjing University, Nanjing 210093, P. R. China, and Department of Chemistry, Jiangsu Institute of Education, Nanjing 210013, P. R. China

Received May 20, 2006

Novel nanosized lead tungstate (PbWO<sub>4</sub>) hollow spindles were successfully synthesized, for the first time, via a Pluronic P123- (EO<sub>20</sub>PO<sub>70</sub>EO<sub>20</sub>) assisted sonochemical process. The triblock copolymer acted as a structure-directing agent and played a key role in the formation of the hollow spindles. An in situ micelle templating mechanism has been proposed for the possible formation mechanism of the hollow nanostructure. The optical properties of the final products were investigated. It is exciting that the as-prepared PbWO<sub>4</sub> hollow structure shows extraordinarily high room-temperature photoluminescence intensity compared to the solid structures.

## Introduction

The development of nano- or micromaterials with size- and shape-controlled morphologies may open new opportunities in exploring material chemical and physical properties.<sup>1</sup> Hollow structures have attracted great attention due to their widespread potential applications in catalysis, drug delivery, lightweight filler, acoustic insulation, photonic crystals,<sup>2</sup> and so on.

Among the many synthetic routes to inorganic hollow structures, template-directed synthesis, with hard templates, such as polymer latex particles,<sup>3</sup> silica spheres,<sup>4</sup> metal nanoparticles,<sup>5</sup> and carbon spheres,<sup>6</sup> and soft templates, such as emulsion droplets,<sup>7,8</sup> micelles,<sup>9</sup> and gas bubbles,<sup>10</sup> has been demonstrated to be an effective approach. The direct self-assembly of building blocks without external templates has also been utilized for generating hollow structures.<sup>11,12</sup> However, the hollow structures obtained are mostly spherical,

polycrystalline shells consisting of primary particles.<sup>13</sup> Recently, some anisotropic hollow inorganic nanostructures with the regular morphologies have been prepared through different synthetic strategies. Examples include octahedral SnO<sub>2</sub>,<sup>14</sup> hexagon-based drums of ZnO,<sup>15</sup> octahedral Cu<sub>2</sub>O nanocages,<sup>16</sup> 18-facet polyhedral Cu<sub>7</sub>S<sub>4</sub> hollow nanocages,<sup>17</sup> etc.

As an inorganic scintillating crystal, lead tungstate (PbWO<sub>4</sub>) is a promising material with potential applications in high-energy physics. Compared to other well-known scintillators, PbWO<sub>4</sub> is most attractive for its high density (8.3 g/cm<sup>3</sup>), short decay time (less than 10 ns for a large part of light output), high-irradiation damage resistance (10<sup>7</sup> rad for undoped and 10<sup>8</sup> rad for La-doped PbWO<sub>4</sub>), interesting excitonic luminescence, thermoluminescence, and stimulated Raman scattering behavior.<sup>18,19</sup> PbWO<sub>4</sub> single crystals have usually been grown from the melt using the Czochralski<sup>20</sup>

\* To whom correspondence should be addressed. E-mail: jjzhu@netra.nju.edu.cn. Phone and fax: +86-25-83594976.

<sup>†</sup> Nanjing University, Nanjing 210093, P. R. China.

<sup>‡</sup> Jiangsu Institute of Education.

- (1) MacLachlan, M. J.; Manners, I.; Ozin, G. A. *Adv. Mater.* **2000**, *12*, 675.
- (2) Caruso, F. *Chem.—Eur. J.* **2000**, *6*, 413.
- (3) Caruso, F.; Caruso, R. A.; Möhwald, H. *Science* **1998**, *282*, 1111.
- (4) Kim, S.-W.; Kim, M.; Lee, W. Y.; Hyeon, T. *J. Am. Chem. Soc.* **2002**, *124*, 7642.
- (5) Liang, H. P.; Zhang, H. M.; Hu, J. S.; Guo, Y. G.; Wan, L. J.; Bai, C. L. *Angew. Chem., Int. Ed.* **2004**, *43*, 1540.
- (6) Sun, X.; Li, Y. *Angew. Chem., Int. Ed.* **2004**, *43*, 3827.
- (7) Putlitz, B. Z.; Landfester, K.; Fischer, H.; Antonietti, M. *Adv. Mater.* **2001**, *13*, 500.
- (8) Bao, J.; Liang, Y.; Xu, Z.; Si, L. *Adv. Mater.* **2003**, *15*, 1832.
- (9) Zhang, D.; Qi, L.; Ma, J.; Cheng, H. *Adv. Mater.* **2002**, *14*, 1499.
- (10) Peng, Q.; Dong, Y.; Li, Y. *Angew. Chem., Int. Ed.* **2003**, *42*, 3027.

- (11) Bigi, A.; Boanini, E.; Walsh, D.; Mann, S. *Angew. Chem., Int. Ed.* **2002**, *41*, 2163.
- (12) Liu, B.; Zeng, H. C. *J. Am. Chem. Soc.* **2004**, *126*, 8124.
- (13) (a) Liang, Z. J.; Susha, A.; Caruso, F. *Chem. Mater.* **2003**, *15*, 3176. (b) Wang, L.; Sasaki, T.; Ebina, Y.; Kurashima, K.; Watanabe, M. *Chem. Mater.* **2002**, *14*, 4827. (c) Kanungo, M.; Deepa, P. N.; Collinson, M. M. *Chem. Mater.* **2004**, *16*, 5535. (d) Dhas, N. A.; Suslick, K. S. *J. Am. Chem. Soc.* **2005**, *127*, 2368. (e) Schmidt, H. T.; Gray, B. L.; Wingert, P. A.; Ostafin, A. E. *Chem. Mater.* **2004**, *16*, 4942. (f) Fujiwara, M.; Shiokawa, K.; Tannaka, Y.; Nakahara, Y. *Chem. Mater.* **2004**, *16*, 5420.
- (14) Yang, H. G.; Zeng, H. C. *Angew. Chem., Int. Ed.* **2004**, *43*, 5930.
- (15) (a) Gao, P. X.; Wang, Z. L. *J. Am. Chem. Soc.* **2003**, *125*, 11299. (b) Jiang, Z. Y.; Xie, Z. X.; Zhang, X. H.; Lin, S. C.; Xu, T.; Xie, S. Y.; Huang, R. B.; Zheng, L. S. *Adv. Mater.* **2004**, *16*, 904.
- (16) Lu, C. H.; Qi, L. M.; Yang, J. H.; Wang, X. Y.; Zhang, D. Y.; Xie, J. L.; Ma, J. M. *Adv. Mater.* **2005**, *17*, 2562.
- (17) Cao, H. L.; Qian, X. F.; Wang, C.; Ma, X. D.; Yin, J.; Zhu, Z. K. *J. Am. Chem. Soc.* **2005**, *127*, 16024.

and Bridgeman<sup>21</sup> methods. Many recent efforts have been devoted to the shape-controlled synthesis of  $\text{PbWO}_4$  micro- and nanocrystals. Various morphologies, including particles, rods, spheres, spindles, dendrites, pagodas, and 18-facet polyhedrons, have been achieved by wet chemical methods.<sup>22–27</sup>

Since single-crystalline  $\text{PbWO}_4$  nanostructures with tailored architectures are expected to show novel properties, it is desirable to fabricate nanophase  $\text{PbWO}_4$  with modulated hollow morphologies to enhance their special performance. In this paper, we report the first synthesis of single-crystalline  $\text{PbWO}_4$  hollow spindles by using P123 ( $\text{EO}_{20}\text{PO}_{70}\text{EO}_{20}$ ) as a structure-directing agent via a facile sonochemical route. It is exciting that the as-prepared  $\text{PbWO}_4$  hollow structure shows extraordinarily intense room-temperature photoluminescence compared to the solid structures.

## Experimental Section

**Materials.** All the reagents used were of analytical purity and used without further purification. The Pluronic amphiphilic triblock copolymer P123 ( $\text{EO}_{20}\text{PO}_{70}\text{EO}_{20}$ ,  $M_{\text{av}} = 5800$ ) was obtained from Aldrich.  $\text{Pb}(\text{CH}_3\text{COO})_2 \cdot 3\text{H}_2\text{O}$ ,  $\text{Na}_2\text{WO}_4 \cdot 2\text{H}_2\text{O}$ , and absolute ethanol were purchased from Shanghai Second Chemical Reagent Factory (Shanghai, China).

**Synthesis.** In a typical procedure, the aqueous solution of  $\text{Pb}(\text{CH}_3\text{COO})_2 \cdot 3\text{H}_2\text{O}$  (1 mL, 0.5 M) was mixed with P123 solution (4  $\text{g} \cdot \text{L}^{-1}$ , 50 mL) to give a clear and homogeneous solution. The mixture was then exposed to high-intensity ultrasound irradiation under ambient air. Another 1 mL of  $\text{Na}_2\text{WO}_4$  (0.5 M) aqueous solution was introduced into the above mixture under ultrasound treatment. Ultrasound irradiation was accomplished with a high-intensity ultrasonic probe (Xinzhì Co., China, JY92-2D, 0.6 cm diameter; Ti-horn, 20 kHz, 60  $\text{W}/\text{cm}^2$ ) immersed directly in the reaction solution, and the total reaction time lasted for 30 min. In the postreaction treatment, the white precipitate was centrifuged at 9000 rpm once with the mother liquid, to separate the powder from the liquid. It was then washed a few times with distilled water and absolute ethanol in sequence and centrifuged at 9000 rpm. The product was finally dried in air.

**Characterization.** The X-ray powder diffraction (XRD) analysis was performed by a Philips X'pert X-ray diffractometer at a scanning rate of  $4^\circ/\text{min}$  in the  $2\theta$  range from  $10$  to  $80^\circ$ , with graphite-monochromatized  $\text{Cu K}\alpha$  radiation ( $\lambda = 0.15418$  nm). Field-emission scanning electron micrographs (FE-SEM) were taken on a LEO-1530VP field-emission scanning electron microscope.

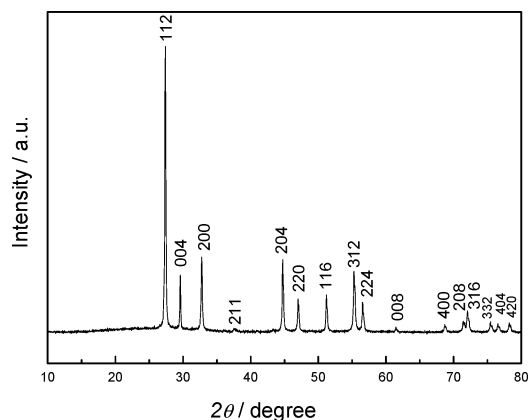


**Figure 1.** XRD pattern of the as-prepared hollow  $\text{PbWO}_4$  sample.

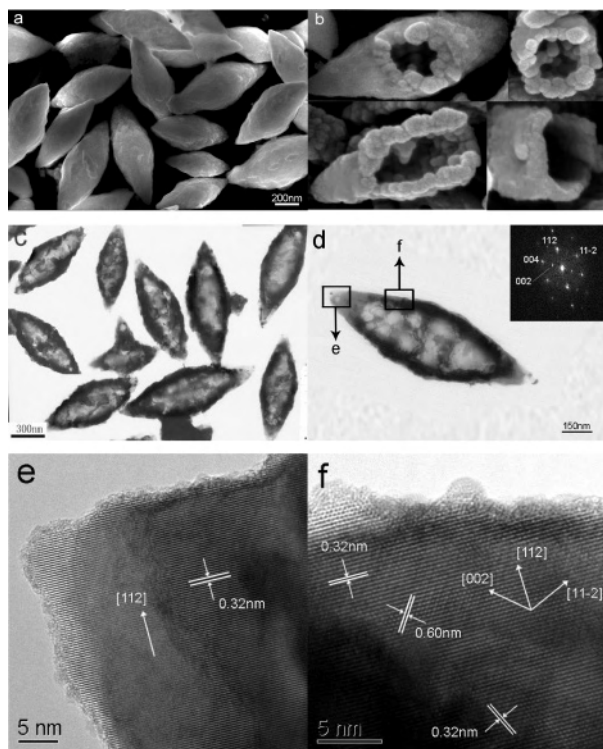
Transmission electron micrographs (TEM) and selected area electron diffraction (SAED) were recorded on a JEOLJEM 200CX transmission electron microscope, using an accelerating voltage of 200 kV. High-resolution transmission electron micrographs (HR-TEM) were obtained by employing a JEOL-2010 high-resolution transmission electron microscope with a 200 kV accelerating voltage. Raman spectra were recorded on a JY HR-800 spectrometer provided by J. Y. Co. at room temperature with an excitation wavelength of 488 nm. Photoluminescence spectra were measured on a SLM48000DSCF/AB2 fluorescence spectrometer made by American SLM Inc. at room temperature.

## Results and Discussion

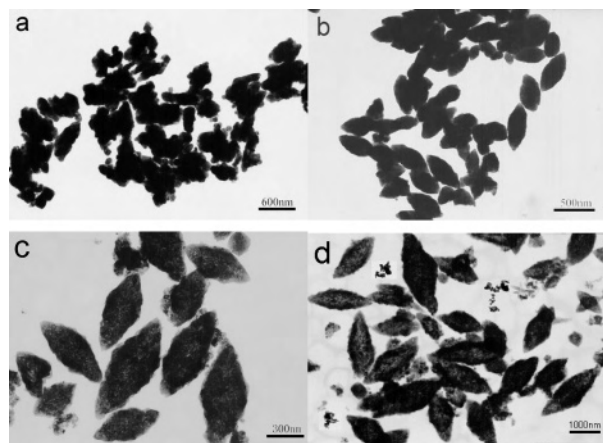
**Characterizations of the Final Products.** Figure 1 shows the XRD pattern of the as-prepared  $\text{PbWO}_4$  sample. All the diffraction peaks can be indexed to a pure tetragonal stolzite structure with cell parameters  $a = 5.46$  and  $c = 12.04$  Å, which are in good agreement with the literature values (JCPDS Card No. 08-0476).

Figure 2a shows a typical SEM image of the as-prepared  $\text{PbWO}_4$  nanocrystals. It is clearly demonstrated that the majority of the crystals have a uniform spindlelike shape with diameter of  $350 \pm 50$  nm at the center and length of about  $900 \pm 100$  nm. A few partly broken hollow spindles can be clearly observed. Figure 2b shows the high-magnification SEM images of several broken hollow spindles viewed from different angles. The morphology and microstructure of the as-synthesized  $\text{PbWO}_4$  crystals were further studied by TEM and HRTEM. As shown in Figure 2c, a strong contrast difference between the edges (dark) and centers (bright) indicates hollow interiors with a wall thickness of about 50 nm. The SAED pattern of the hollow structures shows that the  $\text{PbWO}_4$  hollow structures are single crystals (inset of Figure 2d). HRTEM images provide further insight into their structures. The HRTEM image recorded on the tip of a spindle (Figure 2e) shows well-defined lattice fringes with interplanar spacing of 0.32 nm for the (112) faces of tetragonal  $\text{PbWO}_4$ , indicating the high crystallinity of the product. The HRTEM image obtained on the shell of a spindle (Figure 2f) indicates clear interplanar spacings of 0.32 and 0.60 nm, corresponding to the (112) and (002) crystal faces, respectively. The results of HRTEM and SAED show that the product is high-quality single crystal and the

- (18) Kobayashi, M.; Ishii, M.; Usuki, Y. *Nucl. Instrum. Methods Phys. Res., Sect. A* **1998**, *406*, 442.
- (19) Hara, K.; Ishii, M.; Kobayashi, M.; Nikl, M.; Takano, H.; Tanaka, M.; Tanji, K.; Usuki, Y. *Nucl. Instrum. Methods Phys. Res., Sect. A* **1998**, *414*, 325.
- (20) Nitsch, K.; Nikl, M.; Ganschow, S.; Reiche, P.; Uecker, R. *J. Cryst. Growth* **1996**, *165*, 163.
- (21) Tanji, K.; Ishii, M.; Usuki, Y.; Kobayashi, M.; Hara, K.; Takano, H. *J. Cryst. Growth* **1999**, *204*, 505.
- (22) Liu, B.; Yu, S. H.; Li, L. J.; Zhang, Q.; Zhang, F.; Jiang, K. *Angew. Chem., Int. Ed.* **2004**, *43*, 4745.
- (23) Hu, X. L.; Zhu, Y. J. *Langmuir* **2004**, *20*, 1521.
- (24) Chen, D.; Shen, G. Z.; Tang, K. B.; Liang, Z.; Zheng, H. G. *J. Phys. Chem. B* **2004**, *108*, 11280.
- (25) Geng, J.; Zhu, J. J.; Chen, H. Y. *Cryst. Growth Des.* **2006**, *6*, 321.
- (26) Geng, J.; Zhang, J. R.; Hong, J. M.; Zhu, J. J. *Int. J. Mod. Phys. B* **2005**, *19*, 2734.
- (27) An, C. H.; Tang, K. B.; Shen, G. Z.; Wang, C. R.; Qian, Y. T. *Mater. Lett.* **2002**, *57*, 565.



**Figure 2.** (a) Typical SEM image of the as-prepared PbWO<sub>4</sub> sample. (b) SEM images of several broken hollow spindles viewed from different angles. (c) Typical TEM image and (d) SAED pattern of the product. HRTEM images recorded on (e) the tip and (f) the shell of a hollow spindle.



**Figure 3.** TEM images of PbWO<sub>4</sub> samples prepared under ultrasonic treatment (a) without P123 and (b–d) under different P123 concentrations: (b) 2 g·L<sup>-1</sup>; (c) 3 g·L<sup>-1</sup>; (d) 5 g·L<sup>-1</sup>.

main axis of the hollow structure grew preferentially along the *c* axis. The same crystal direction of (112) faces can be observed in the different regions of the spindle, which suggests that the sample is structurally uniform with an oriented crystallographic direction.

**Effect of P123 Concentration.** The copolymer concentration has a great effect on the formation of hollow PbWO<sub>4</sub> crystals. When the experiment was carried out without the P123 copolymer, while keeping other experimental conditions unchanged, only product with irregular shape was obtained (Figure 3a). PbWO<sub>4</sub> crystals have also been synthesized at varied polymer concentrations for comparison. The product obtained at a lower polymer concentration,

namely, 2 g·L<sup>-1</sup>, is composed of a spindle-like solid structure (Figure 3b). As the polymer concentration was increased to 3 g·L<sup>-1</sup>, the product exhibited loose spindles, which showed many inner pores on the surfaces with sizes less than 10 nm (Figure 3c). Increasing the polymer concentration to 4 g·L<sup>-1</sup> resulted in the formation of the hollow PbWO<sub>4</sub> nanospindles shown in Figure 2. If the polymer concentration was further increased to 5 g·L<sup>-1</sup>, the product was a mixture of PbWO<sub>4</sub> larger hollow spindles and some solid particles (Figure 3d).

The experimental results indicated that the triblock copolymer played a key role in the formation of PbWO<sub>4</sub> hollow structure. P123 possesses a long PPO segment and two medium-length PEO blocks and has a relatively high molecular weight ( $M_{av} = 5800$ ). Such a combination favors the formation of micelles, which have dehydrated PPO blocks in their cores and coronas of hydrated PEO segments at the micellar surface, when the polymer concentration exceeds the critical micelle concentration (cmc) in aqueous solution.<sup>28</sup> PEO in PEO–PPO–PEO block copolymers is known to form cavities similar to those of crown ethers (pseudo-crown ether structure) that are able to bind with metal ions.<sup>29,30</sup> The induced cyclization is caused by ion–dipole interactions between the template ion and the electron lone pairs of the ethylene oxide linkages.<sup>31,32</sup> Cavities can be formed by an individual polymer molecule and also by participation of several polymers.<sup>29–32</sup> An increase in polymer concentration enhances cavity formation by bringing several polymers closer together, which leads to the formation of large P123 aggregates or clusters of P123 micelles in the solution.<sup>28</sup> Because the size of the obtained PbWO<sub>4</sub> hollow interiors (several hundred of nanometers) was much bigger than that of single P123 micelles in solution (tens of nanometers),<sup>33,34</sup> it appears that the hollow spindles were formed not by directly templating the original P123 micelles but by templating dynamic templates such as larger P123 aggregates formed during the precipitation process due to the interaction between the polymer and various inorganic species.

When the concentration of P123 is below the critical micelle concentration (2 g·L<sup>-1</sup>, 20 °C),<sup>35</sup> the copolymer chains exist as single chains and might only work as a capping reagent. The preferential adsorption mechanism is predominant leading to the formation of solid spindles. When the P123 concentration is higher than the cmc, the core–shell micelles form and the template mechanism is dominant. With different concentrations of P123, the micelle shape would also change and subsequently leads to the formation

- (28) For a comprehensive review, see: Alexandridis, P.; Hatton, T. A. *Colloids Surf., A* **1995**, *96*, 1.  
 (29) Warshawsky, A.; Kalir, R.; Deshe, A.; Berkovitz, H.; Patchornik, A. *J. Am. Chem. Soc.* **1979**, *101*, 4249.  
 (30) Elliott, B. J.; Scranton, A. B.; Cameron, J. H.; Bowman, C. N. *Chem. Mater.* **2000**, *12*, 633.  
 (31) Liu, K. J. *Macromolecules* **1968**, *1*, 308.  
 (32) Yanagida, S.; Takahashi, K.; Okahara, M. *Bull. Chem. Soc. Jpn.* **1977**, *50*, 1386.  
 (33) Nagarajan, R. *Colloids Surf., B* **1999**, *16*, 55.  
 (34) Kabanov, A. V.; Nazarova, I. R.; Astafieva, I. V.; Batrakova, E. V.; Alakhov, V. Y.; Yaroslavov, A. A.; Kabanov, V. A. *Macromolecules* **1995**, *28*, 2303.  
 (35) Alexandridis, P.; Holzwarth, J. F.; Hatton, T. A. *Macromolecules* **1994**, *27*, 2414.

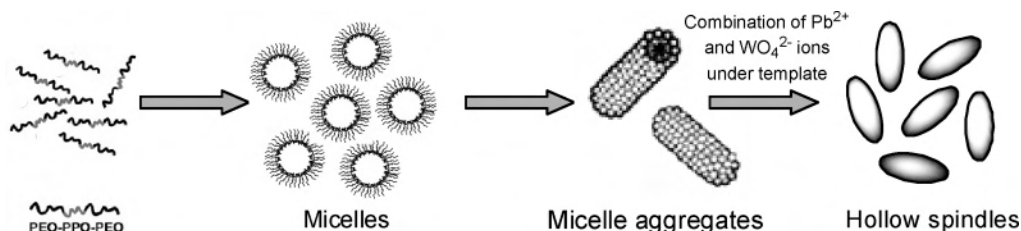


**Figure 4.** Schematic illustration of the formation of  $PbWO_4$  hollow spindles under ultrasonic treatment.

of crystals with different morphologies. It was expected that when P123 concentration was increased from 2 to 4  $g \cdot L^{-1}$ , the probability for the formation of large P123 aggregates would increase, leading to the transition of the  $PbWO_4$  products from solid spindles through loose spindles to hollow spindles. However, when the P123 concentration was increased to 5  $g \cdot L^{-1}$ , in addition to the formation of larger hollow spindles, some small  $PbWO_4$  solid particles would also appear (Figure 3d) as the result of excessive adsorption of P123 on the surfaces of  $PbWO_4$  nuclei preventing their further growth. In short, the complex micellar aggregates formed by P123 and lead acetate acted as temporary soft templates for the formation of the hollow  $PbWO_4$  spindles. This micellar templating formation process is somewhat similar to that of  $PbTe$  nanobox<sup>36</sup> and inorganic hollow spheres.<sup>37–39</sup>

**Effect of Ultrasound Irradiation and Possible Growth Mechanism.** It has been well established that the ultrasonic irradiation introduces a variety of physical and chemical effects deriving from acoustic cavitation.<sup>40</sup> Such cavitation behavior, i.e., the formation, growth, and implosive collapse of bubbles, has been used extensively to generate novel materials with unusual properties. And also, the ultrasonic irradiation method is an effective method to induce emulsification and the formation of vesicles in the liquid–liquid heterogeneous system as widely found in studies.<sup>41</sup> Here, ultrasound irradiation also played an important role and is found to be necessary to the synthesis of hollow structure. Comparative experiments under vigorous electric stirring instead of ultrasonic treatment only obtained solid spindles (see Supporting Information, Figure S1). So the ultrasound wave might urge the initial self-aggregation of P123 molecules to form different sized micellar aggregates directly determining the texture of the spindles, as have been similarly reported in some literature.<sup>37–38,42</sup> Gedanken's group has established sonochemical route to produce some tubular assemblies and a variety of mesoporous oxide materials.<sup>43</sup> The advantage of the application of ultrasound irradiation

to the synthesis of mesoporous materials is the significant reduction in fabrication time and the possibility to induce the aggregation of nanoparticles without destroying the micellar structure.<sup>44</sup> In the present case, the role of sonication is not only to accelerate the reaction between the raw materials but also to lead to the growth and crystallization of  $PbWO_4$  due to the extreme conditions.<sup>45</sup> Ultrasound appears to be particularly effective as a means of inducing nucleation and may influence crystallization through the mechanisms of cavitation and acoustic streaming,<sup>46</sup> which is responsible for the formation of final single-crystalline  $PbWO_4$  product.<sup>47,48</sup>

In this case, the sonication time of 30 min is necessary for the formation of final hollow spindles. We have also carried out experiments by prolonging the sonication time. It was observed that the dimensions of  $PbWO_4$  nanospindles increased gradually with the prolongation of sonication time to 1 h and the morphology became less uniform (see Supporting Information, Figure S2a). With the increasing sonication time to 2 h, the surface of the initial hollow spindles became coarse and some of the spindles fell to irregular small pieces (see Supporting Information, Figure S2b). This may be related to the surface corrosion and fragmentation of solids in the presence of high-intensity ultrasound irradiation. For brittle materials, especially layered inorganic sulfides and oxides, interparticle collisions can induce fragmentation.<sup>40b</sup>

On the basis of the experimental results, a possible formation mechanism is proposed in Figure 4.  $PbWO_4$  hollow spindles can be formed by templating the P123 micellar aggregates induced by the ultrasonic irradiation. The as-formed micellar aggregates are metastable and characterized by active ligands on the surface, which act as temporary templates during the formation of hollow structure.  $Pb^{2+}$  ions in the solution are easily attracted on the micellar surfaces by forming  $Pb-(PEO-PPO-PEO)$  units. Thus, the  $Pb^{2+}$  ion-covered micelles can be formed, which provide nucleation domains for the subsequent reaction between  $Pb^{2+}$  and

(36) Wang, W. Z.; Poudel, B.; Wang, D. Z.; Ren, Z. F. *Adv. Mater.* **2005**, *17*, 2110.

(37) Wang, S. F.; Gu, F.; Lü, M. K. *Langmuir* **2006**, *22*, 398.

(38) Ma, Y. R.; Qi, L. M.; Ma, J. M.; Cheng, H. M.; Shen, W. *Langmuir* **2003**, *19*, 9079.

(39) Hu, J. S.; Guo, Y. G.; Liang, H. P.; Wan, L. J.; Bai, C. L.; Wang, Y. C. *J. Phys. Chem. B* **2004**, *108*, 9734.

(40) (a) Suslick, K. S., Ed. *Ultrasound: Its Chemical, Physical and Biological Efforts*; VCH: Weinheim, Germany, 1988. (b) Suslick, K. S. *Annu. Rev. Mater. Sci.* **1999**, *29*, 295.

(41) (a) Ringsdorf, H.; Schlarb, B.; Venzmer, J. *Angew. Chem., Int. Ed. Engl.* **1988**, *27*, 113. (b) Marques, E. F. *Langmuir* **2000**, *16*, 4798.

(42) Zheng, X. W.; Xie, Y.; Zhu, L. Y.; Jiang, X. C.; Yan, A. H. *Ultrason. Sonochem.* **2002**, *9*, 311.

(43) (a) Gedanken, A.; Tang, X. H.; Wang, Y. Q.; Perkas, N.; Koltypin, Y.; Landau, M. V.; Vradman, L.; Herskowitz, M. *Chem.—Eur. J.* **2001**, *7*, 4546. (b) Wang, Y. Q.; Yin, L. X.; Gedanken, A. *Ultrason. Sonochem.* **2002**, *9*, 285. (c) Zhu, Y. C.; Li, H. L.; Koltypin, Y.; Hacoheh, Y. R.; Gedanken, A. *Chem. Commun.* **2001**, 2616.

(44) Salkar, R. A.; Jeevanandam, P.; Aruna, S. T.; Koltypin, Yu.; Palchik, O.; Gedanken, A. *J. Phys. Chem. B* **2000**, *104*, 893.

(45) Suslick, K. S.; Choe, S. B.; Cichowlas, A. A.; Grinstaff, M. W. *Nature* **1991**, *353*, 414.

(46) Young, F. R. *Cavitation*; McGraw-Hill: New York, 1989.

(47) Zhang, J. L.; Du, J. M.; Han, B. X.; Liu, Z. M.; Jiang, T.; Zhang, Z. F. *Angew. Chem., Int. Ed.* **2006**, *45*, 1116.

(48) Rucroft, G.; Hipkiss, D.; Ly, T.; Maxted, N.; Cains, P. W. *Org. Process Res. Dev.* **2005**, *9*, 923.

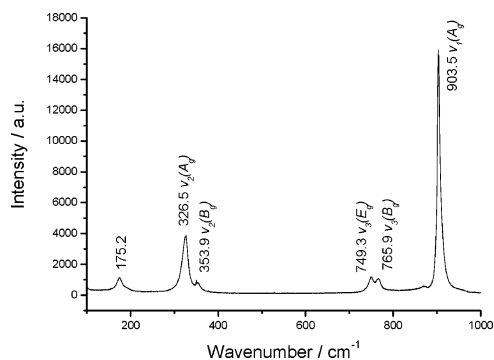


**Figure 5.** Raman spectrum of the hollow PbWO<sub>4</sub> nanospindles.

WO<sub>4</sub><sup>2-</sup> to form PbWO<sub>4</sub> nanoparticles. With the reaction proceeding, the formed PbWO<sub>4</sub> nanoparticles undergo mineralization to form a relatively compact PbWO<sub>4</sub> layer on the surface of the micellar aggregates. The micellar templates can be successfully extracted by the washing process without destroying the spindle structures. This method might also be of potential to synthesize other hollow nanostructured functional materials by reacting with appropriate compounds.

**Raman Spectra.** The optical properties of the as-prepared products were also studied. The Raman spectrum of the stolzite hollow structure (Figure 5) shows six bands in the range of 100–1000 cm<sup>-1</sup>. The peaks located at 903.5, 765.9, 749.3, 353.9, and 326.5 cm<sup>-1</sup> correspond to the vibration modes ν<sub>1</sub>(A<sub>g</sub>), ν<sub>3</sub>(B<sub>g</sub>), ν<sub>3</sub>(E<sub>g</sub>), ν<sub>2</sub>(B<sub>g</sub>), and ν<sub>2</sub>(A<sub>g</sub>), respectively, which are consistent with those reported previously.<sup>49,50</sup> The peak at 175.2 cm<sup>-1</sup> was not assigned by Ross,<sup>50</sup> but Griffith, Yu, and our research team have observed a similar peak in synthetic stolzite samples<sup>22,25,51</sup> and this peak could be assigned as the translational mode of the WO<sub>4</sub> group analogous to that for CdMoO<sub>4</sub>.<sup>49</sup>

**Photoluminescence Properties.** Figure 6a shows the room-temperature photoluminescence spectrum of the hollow nanostructure using the excitation line at 300 nm. The spectrum shows that the sample has a typical blue emission peak at about 450 nm. It is interesting that the PL intensity of the hollow structure is much higher than that of loose and solid spindle structures (as shown in Figure 6b,c) prepared under different P123 concentrations (2 and 3 g·L<sup>-1</sup>, respectively). And the blue emission peak of the hollow

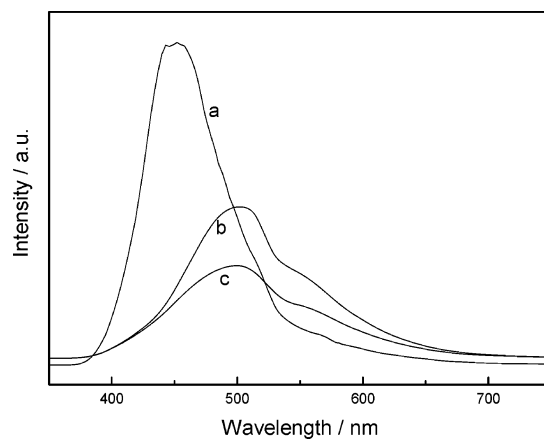


**Figure 6.** Room-temperature PL spectra of (a) as-prepared hollow PbWO<sub>4</sub> sample, (b) loose spindles prepared in a 3 g·L<sup>-1</sup> P123 system, and (c) solid spindles prepared in a 2 g·L<sup>-1</sup> P123 system.

structure differs from the typical green one obtained from the solid spindles (peak at about 500 nm).<sup>52</sup> These results indicate that luminescence properties of PbWO<sub>4</sub> are very sensitive for its structure and strongly dependent on structural defects. These hollow crystals are expected to exhibit high light-collection efficiency and enhanced luminescence performance due to their hollow structures and large internal surface area at their interior.<sup>53</sup> The greatly enhanced luminescence performance observed in the hollow nanostructure is exciting and may have significant technological applications in the inorganic scintillating field.

## Conclusion

In summary, the PbWO<sub>4</sub> hollow structure has been successfully synthesized by using P123 as soft template via a facile sonochemical route. The experimental results showed that surfactant P123 and ultrasound irradiation played key roles in the formation of hollow spindles. The as-prepared hollow PbWO<sub>4</sub> structure is highly crystalline single crystal and exhibits blue emission with excitingly high intensity. This unique hollow PbWO<sub>4</sub> structure may be a promising candidate for both fundamental research and functional applications.

**Acknowledgment.** This work is supported by the National Natural Science Foundation of China (Grant Nos. 20325516, 90206037, and 20521503). We thank Professor Guobing Ma for his skillful measurement on SEM and Professor Yinong Lv for his skillful measurement on HRTEM.

**Supporting Information Available:** Comparative experimental results under vigorous electric stirring, effect of sonication time and concentrations of Pb(CH<sub>3</sub>COO)<sub>2</sub> and Na<sub>3</sub>WO<sub>4</sub> on the final products. This material is available free of charge via the Internet at <http://pubs.acs.org>.

IC0608804

(49) Crane, M.; Frost, R. L.; Williams, P. A.; Kloprogge, J. T. *J. Raman Spectrosc.* **2002**, *33*, 62.

(50) Ross, S. D. *Inorganic Infrared and Raman Spectra*; McGraw-Hill: Maidenhead, U.K., 1972.

(51) Bastians, S.; Crump, G.; Griffith, W. P.; Withnall, R. *J. Raman Spectrosc.* **2004**, *35*, 726.

(52) Nikl, M. *Phys. Status Solidi A* **2000**, *178*, 595.

(53) (a) Gou, L. F.; Murphy, C. J. *Nano Lett.* **2003**, *3*, 231. (b) Grätzel, M. *Nature* **2001**, *414*, 338. (c) Huynh, W. U.; Dittmer, J. J.; Alivisatos, A. P. *Science* **2002**, *295*, 2425. (d) Nishimura, S.; Abrams, N.; Lewis, B. A.; Halaoui, L. I.; Mallouk, T. E.; Benkstein, K. D.; Lagemaat, J. V.; Frank, A. J. *J. Am. Chem. Soc.* **2003**, *125*, 6306.